Eur Biophys J (1987) 15: 225–230

European Biophysics Journal

The active site of Manganese-containing superoxide dismutase from *Bacillus stearothermophilus* studied by ^{1}H and ^{19}F magnetic relaxation

P. Viglino [1] *, E. F. Orsega [1], E. Argese [2], R. Stevanato [1], and A. Rigo [3]

[1] Department of Spectroscopy, Electrochemistry and Physical Chemistry, University of Venice, I-30100 Venice, Italy
[2] Department of Environmental Sciences, University of Venice, I-30100 Venice, Italy
[3] Laboratory of Biophysics, Institute of Biological Chemistry, University of Padua, I-35100 Padua, Italy

Received August 2, 1986/Accepted in revised form May 26, 1987

Abstract. The dependence of the magnetic relaxation rates of ^{1}H and $^{19}F^-$ on temperature, frequency, pH and N_3^- concentration, were measured in solutions of Manganese-containing superoxide dismutase of *Bacillus stearothermophilus*, and were compared to activity measurements, in order to obtain some information on the structure and dynamics at Mn(III) present in the active site of the enzyme. The experimental data lead us to hypothesize the presence of two binding sites in the coordination sphere of the enzyme bound Mn(III), which are accessible to water and anions and have different chemical and spectroscopic properties. NMR measurements carried out in the presence of competitive inhibitors and the pH dependence of both NMR relaxation rates suggest that F^-, N_3^- and OH^- ions bind to one site, while a water molecule binds to the other one. The stability constant values of the complexes between these anions and the enzyme are reported. The influence of the anions on activity and the pH dependence of NMR parameters are discussed.

Key words: Mn superoxide dismutase, NMR relaxation, pH influence on enzyme structure

Introduction

Manganese containing superoxide dismutase, (EC. 1.15.1.1) are a class of metalloenzymes which catalyse the reaction

$$2\,O_2^- \xrightarrow[H^+]{\text{MnSOD}} H_2O_2 + O_2$$

according to an oxidation-reduction cycle different from the simple two step mechanism found for copper containing superoxide dismutases (Pick et al. 1974; McAdam et al. 1977a, b). These enzymes show a dimeric structure and contain manganese as functional metal ion, which, in the enzyme resting state, is present as Mn(III) (Fee et al. 1976; Walker et al. 1980; Brock and Walker 1980). Though many reports discuss the properties of these enzymes, there are only few studies on the active site structure (Stalling et al. 1985). In particular, nuclear proton magnetic resonance measurements were used to obtain information on the structure, equilibria and dynamics of the active site of Mn-SOD from *Escherichia coli* (Villafranca et al. 1974).

In the present work the nuclear magnetic relaxation rates of water protons and of $^{19}F^-$ have been measured and have been correlated with activity measurements in order to further characterize the active site of manganese superoxide dismutase from *Bacillus stearothermophilus*.

Materials and methods

All chemicals were reagent grade and were used without further purification. The MnSOD was prepared according to Brock et al. (1976).

Before NMR experiments the enzyme was dialyzed against 5 m*M* sodium phosphate, pH 7.4. The enzyme concentration was calculated using $A_{280}^{1\%} = 13.2$ (McAdam et al. 1977a). A value of 1.02 atoms of Mn per molecule was calculated from absorbance measurements at 480 nm, $\varepsilon = 650\,M^{-1}\,cm^{-1}$ (McAdam et al. 1977a), while 1.05 atoms of Mn per molecule of enzyme were calculated from the double integration of EPR spectra of the Mn^{++} aquoion obtained by heating the enzyme with concentrated HNO_3.

^{19}F and proton relaxation measurements were carried out on a pulsed NMR apparatus operating at 7, 16 and 27 MHz, as previously reported (Viglino et al. 1979). The longitudinal relaxation time, T_1, was measured using either $90° - \tau - 90°$ or $180° - \tau - 90°$ sequences. The transverse relaxation time, T_2, was obtained from the Carr-Purcell sequence with

* To whom offprint requests should be sent
Abbreviations: MnSOD, Manganese containing superoxide dismutase

Gill-Meiboom modification. The paramagnetic contributions to the relaxation rates, (T_{1p}^{-1}) and (T_{2p}^{-1}), of protons and ^{19}F were calculated by subtracting the diamagnetic contribution, measured in the presence of the apoenzyme, from the corresponding experimental T_1^{-1} and T_2^{-1}. The apoenzyme was prepared following the procedure reported by Brock and Walker (1980). The apoenzyme shows an activity less than 1% of that of the native enzyme and does not contribute significantly to proton and ^{19}F relaxation rates.

If not otherwise stated, the experiments were performed at 16 MHz, 23 °C and in the presence of 10^{-4} *M* EDTA to avoid the effects of paramagnetic impurities on the relaxation times.

Activity measurements were carried out with the assay based on the competition between MnSOD and Cytochrome C for the flux of O_2^- generated by the Xantine oxidase reaction (McCord and Fridovich 1969).

Results

^{19}FMR data

The paramagnetic contributions to the longitudinal and transverse relaxation rates of ^{19}F are very sensitive to the presence of MnSOD. In fact the ^{19}F molar relaxivity (R_F), in 0.5 *M* F^- solution is given by:

$$R_F = T_{1p}^{-1}\,[\text{MnSOD}]^{-1}$$
$$= 2.9 \times 10^6\, M^{-1}\,s^{-1} \text{ at pH } 7.5\,.$$

This high relaxivity value, very close to that found for Cu, Zn superoxide dismutase (Viglino et al. 1979), clearly indicates a direct binding of F^- ion at Mn(III) present in the active site. Moreover, as previously described (Viglino et al. 1979), the straight lines obtained when plotting T_{1p} vs. $[F^-]$ at pH 7.5 and pH 10.5 (correlation coefficients $r = 0.998$ and $r = 0.999$ respectively) indicate a 1:1 interaction between fluoride ion and the enzyme bound Mn, according to the reaction scheme:

$$E + F^- \underset{}{\overset{K_F}{\rightleftharpoons}} EF\,,$$

where E is the free enzyme, EF is the complex F^--enzyme and K_F is the stability constant of the complex.

Under our experimental conditions, where $[F^-] \gg [EF]$, the following relationships (Luz and Meiboom 1964; Dwek 1973), can be written:

$$T_{1,2p}^{-1} = [EF]/[F^-](T_{1,2M} + \tau_M)$$
$$= E_0/(K_F^{-1} + [F^-])\,(T_{1,2M} + \tau_M)$$

where $T_{1,2M}$ is the relaxation time of the fluoride ion bound to the enzyme, τ_M the correlation time of the chemical exchange between the fluoride ion bound to the enzyme and the bulk of the solution, and E_0 the total enzyme concentration. These equations allow us to propose the use of ^{19}F as a probe of the structural and dynamic features of the enzyme active site. To this purpose measurements of $T_{1,2p}$ at different frequencies and temperatures were performed. From the plots of $T_{1,2p}^{-1}$ vs. the reciprocal of the temperature of Fig. 1, at neutral and alkaline pH values, we calculated (Dwek 1973), limits for τ_M, see Table 1, and the lower value for the activation enthalpy of the chemical exchange process, which resulted $\Delta H > 4.0$ Kcal M^{-1} at pH 7.5.

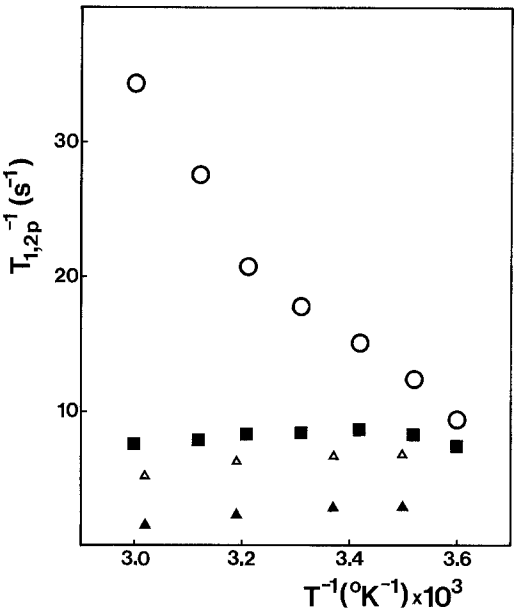

Fig. 1. Temperature dependence of nuclear magnetic relaxation rates of ^{19}F in 0.5 *M* KF. ○, T_{2p}^{-1}, 3 μ*M* MnSOD in 0.1 *M* phosphate, pH 7.5; ■, T_{1p}^{-1}, 3 μ*M* MnSOD in 0.1 *M* phosphate, pH 7.5; △, T_{2p}^{-1}, 2.1 μ*M* MnSOD in 0.1 *M* carbonate, pH 10.5; ▲, T_{1p}^{-1}, 2.1 μ*M* MnSOD in 0.1 *M* carbonate, pH 10.5

The frequency dependence of the relaxation rates, see Table 2, agrees with a T_{2p}^{-1} controlled by τ_M at 16 MHz and pH 7.5, however a full analysis of the data of Table 1 in terms of Solomon-Bloembergen-Morgan theory is not possible because of the lack of data on the zero-field-splitting parameters (D and E) and on the different electron relaxation times of Mn(III), characterized by $S = 2$ and $I = 5/2$. In this regard, non negligible D values have been attributed to Mn(III); for instance a D value in the range $1 - 2\ cm^{-1}$ has been estimated for the MnSOD from *Escherichia coli* (Fee et al. 1976), while values of $D = 3.4\ cm^{-1}$ and $E = 0.116\ cm^{-1}$ have been found for Mn doped TiO_2 (Gerritzen and Sabisky 1963). These data, and the absence of a detectable EPR spectrum of MnSOD, indicate a large zero-field splitting and short electron spin relaxation times ($\tau_s < 10^{-11}$ s) for the enzyme Mn(III).

Table 1. Relaxation time parameters determined from ^1H and ^{19}F NMR data at 16 MHz. The concentration of MnSOD was 3.2 μM in 0.5 M KF for ^{19}F relaxation time measurements and 0.14 mM for ^1H relaxation time measurements

Nucleus	pH	T_{1p}^{-1}	T_{2p}^{-1}	τ_M	T_{1M}	T_{2M}	K_F	K_{N_3}	K_{OH}
		[s^{-1}]	[s^{-1}]	[$s \times 10^7$]	[$s \times 10^7$]	[$s \times 10^7$]	[M^{-1}]	[M^{-1}]	[M^{-1}]
^{19}F	7.5	9.3	16.6	> 2	< 2.8	< 0.7	4.5	19	11,300[a]
^{19}F	10.5	4.4	10.0	< 2	> 8	> 2.6	5	12	9,500
^1H	7.5	0.39	0.56	< 20	> 45	> 25	–	–	11,000[a]
^1H	10.5	1.00	1.24	–	–	–	4.7	13	9,500

[a] This K_{OH} value holds up to pH 10.3

Table 2. Frequency dependence of ^1H and ^{19}F relaxation times at pH 7.5. The concentration of MnSOD was 3.2 μM in 0.5 M K_F for ^{19}F relaxation time measurements and 0.14 mM for ^1H relaxation time measurements

Frequency (MHz)	$^{19}F\ T_{1p}^{-1}$ [s^{-1}]	$^{19}F\ T_{2p}^{-1}$ [s^{-1}]	$^1H\ T_{1p}^{-1}$ [s^{-1}]	$^1H\ T_{2p}^{-1}$ [s^{-1}]
7	11.6	14.6	0.36	0.44
16	9.3	16.6	0.39	0.56
27	6.6	16.5	0.40	0.57

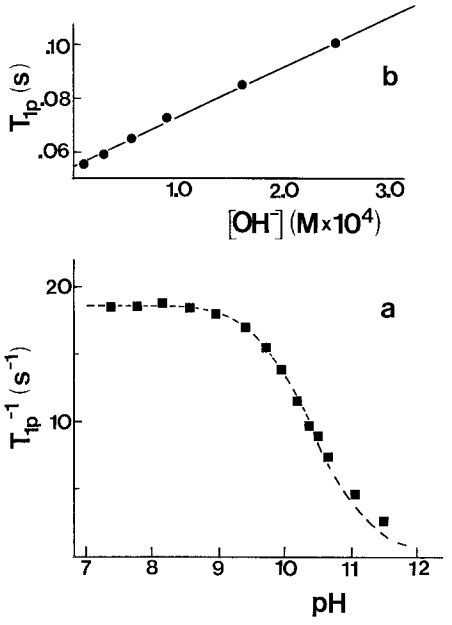

Fig. 2a and b. pH dependence of ^{19}F longitudinal relaxation rate. **a** ■, T_{1p}^{-1}, 6.4 μM MnSOD in 0.5 M KF, the *broken line* is the theoretical fit according to Eq. (1), the pH of the solutions was kept constant with 0.1 M phosphate or borate or carbonate buffers. **b** ●, linearization of relaxation data of **a** according to Eq. (1)

The ^{19}F relaxation rates are strongly influenced by addition of N_3^- or OH^-. In fact measurements carried out both at pH 7.5 and pH 10.5 in the presence of increasing amounts of azide, up to 1 M, show a strong decrease of $^{19}F\ T_{1p}^{-1}$. Similarly $^{19}F\ T_{1p}^{-1}$ measured at

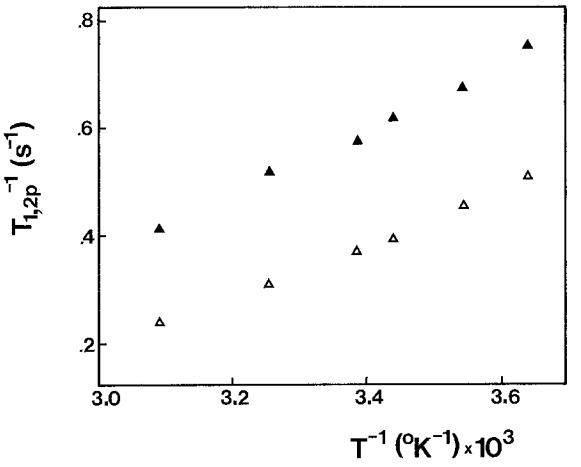

Fig. 3. Temperature dependence of nuclear magnetic relaxation rates of protons. The concentration of MnSOD was 0.14 mM in 0.1 M phosphate, pH 7.5. ▲, T_{2p}^{-1}; △, T_{1p}^{-1}

different pH values, in the absence of azide and at constant ionic strength, shows an appreciable and reversible decrease, above pH 9, which becomes irreversible above pH 11.5, see Fig. 2a. All these measurements could be interpreted in terms of 1 : 1 competitive inhibition between F^- and OH^- or N_3^- for the MnSOD active site because straight lines are obtained when $^{19}F\ T_{1p}$ values are plotted vs. $[N_3^-]$ or $[OH^-]$ (Viglino et al. 1979), see e.g. Fig. 2b and also the Discussion.

PMR data

The temperature dependence of the proton relaxation rates of water solutions of MnSOD at pH 7.5, reported in Fig. 3, shows a positive slope which supports fast exchange conditions, i.e. $T_{1M}, T_{2M} > \tau_M$ (Dwek 1973). From this figure an apparent activation energy of about 1 Kcal mol^{-1} has been calculated for both proton relaxation processes. The low values of the activation energies suggest that T_{1M} and T_{2M} are governed by τ_s through τ_c, and the frequency dependence at 7, 16 and 27 MHz, see Table 2, do not contradict this state-

ment. However, we cannot go far with the analysis of the experimental data for the same reasons as in the case of ^{19}FMR data.

The data of Fig. 4, which show the increase of proton longitudinal relaxation rate at increasing pH values, are more interesting for gaining an understanding of the interactions occurring at the active site of MnSOD. Moreover the inhibition of proton T_{1p}^{-1} by F^- and N_3^- is pH dependent. In fact at pH 7.5 the addition of 1 M F^- does not affect the proton T_{1p}^{-1}, though ^{19}F is strongly relaxed by MnSOD, while at higher pH values an increasing effect of F^- takes place, see Fig. 4. At pH 10.5, for instance, the T_{1p}^{-1} value decreases asymptotically upon increasing the concentration of F^-, see Fig. 5. This asymptotic value cannot be measured directly since the low value of the stability constant K_F, see Table 1, would require F^- concentrations much higher than 1 M. However by extrapolation of the experimental data of Fig. 5 it was possible to calculate a value $(T_{1p}^{-1})_\infty$ for the asymptote.

The difference $(T_{1p}^{-1})_* = T_{1p}^{-1} - (T_{1p}^{-1})_\infty$ is proportional to the concentration of the free enzyme and can be correlated with the concentration of fluoride. In fact the plot of $(T_{1p})_*$ vs. $[F^-]$ is a straight line only for a defined value of $(T_{1p}^{-1})_\infty$ according to the model of 1 : 1 competitive binding in the first coordination sphere of an enzyme active centre.

Analogous results have been obtained in the case of N_3^-, see Fig. 6, with the $(T_{1p}^{-1})_\infty$ value being smaller than that measured in solutions containing F^-, over the pH range explored.

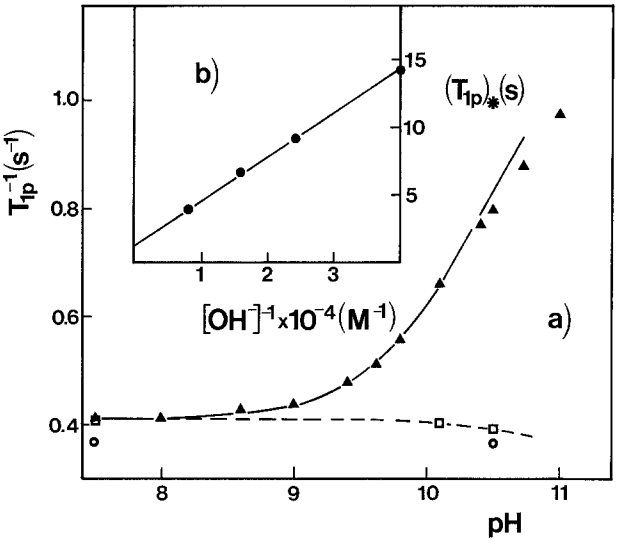

Fig. 4a and b. Dependence of proton longitudinal relaxation rates on pH, F^- and N_3^-. The concentration of MnSOD was 0.2 mM; the pH of the solutions was kept constant with 0.1 M phosphate or borate or carbonate buffers. **a** ▲, T_{1p}^{-1} in the presence of 0.5 M KF, the *full line* is the theoretical fit according to Eq. (2); □, (T_{1p}^{-1}) in the presence of saturating KF; the *broken line* is the fit of the $(T_{1p}^{-1})_\infty$ values in the presence of saturating KF; ○, (T_{1p}^{-1}) in the presence of saturating NaN_3. **b** ●, linearization of $(T_{1p}^{-1})_*$ in the presence of 0.5 M KF, according to Eq. (2)

Activity measurements

MnSOD activity measurements were performed in the presence of increasing amounts of F^- or N_3^- at pH 7.8. The experiments carried out in the presence of increasing N_3^- concentration show a progressive inhibition of the enzyme activity. For instance 20 and 33 mM N_3^- reduced MnSOD activity to 50% and to 35% respectively, in good agreement with the literature data (Misra and Fridovich 1978).

Fluorine ion was found to be a less effective inhibitor; for instance 100 mM F^- reduced the MnSOD activity to 55% of the original value.

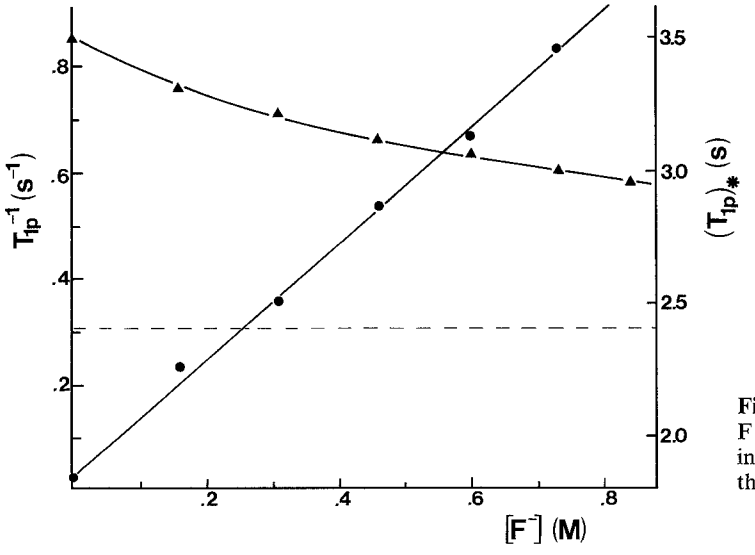

Fig. 5. Dependence of proton longitudinal relaxation rate on F^- concentration. The concentration of MnSOD was 0.16 mM in 0.1 M carbonate, pH 10.5; ▲, T_{1p}^{-1}, the *broken line* represents the asymptotic value $(T_{1p}^{-1})_\infty$; ●, $(T_{1p}^{-1})_* = [T_{1p}^{-1} - (T_{1p}^{-1})_\infty]^{-1}$

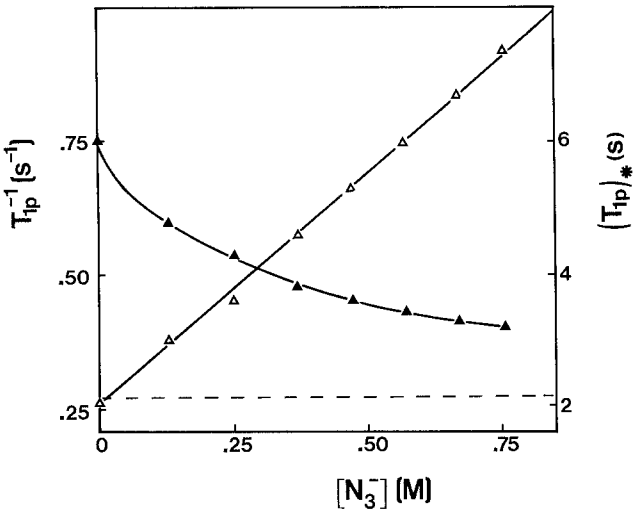

Fig. 6. Dependence of proton longitudinal relaxation rate on N_3^- concentration. The concentration of MnSOD was 0.14 m*M* in 0.1 *M* carbonate, pH 10.5; ▲, T_{1p}^{-1}, the *broken line* represents the asymptotic value $(T_{1p}^{-1})_\infty$; △, $(T_{1p})_* = [T_{1p}^{-1} - (T_{1p}^{-1})_\infty]^{-1}$

Discussion

A comprehensive though approximate elaboration of the NMR experimental data lead us to calculate some interesting parameters at 16 MHz, which are reported in Table 1, for comparison purposes. These data show clearly the direct binding of both water and fluoride ion in the first coordination sphere of Mn(III) present in the active site. Moreover the analysis of the PMR data, see Figs. 4, 5 and 6, suggests that, at least at alkaline pH values, the proton relaxation rate, in the presence of MnSOD, is the sum of two different components: the first, which corresponds to $(T_{1p}^{-1})_\infty$, obtained after saturating additions of F^-, should be ascribed to a water molecule at a site we call *A*; the second, which corresponds to $(T_{1p}^{-1})_*$, inhibited by F^- and N_3^-, should be ascribed to the binding to a second site on Mn(III) we call *B*. According to our experimental data the two sites exchange with the bulk of the solution; the proton relaxivity at site *A* appearing almost pH independent, while the one at site *B*, negligible at neutral pH, strongly increases with pH. The comparison of the opposite trends of ^{19}F and proton T_{1p}^{-1} vs. pH, showed in Figs. 2 and 4 respectively, suggests that this different behaviour results from the effect of OH^- anion binding to site *B*. In fact the progressive decrease of the ^{19}F relaxation rate, when the pH is brought from neutral to basic values, can be explained in terms of direct competition between OH^- and F^- for site *B*, where N_3^- also binds. On the basis of this hypothesis the proton relaxation $(T_{1p}^{-1})_*$, previously described, at site *B*, should be due to OH^- binding. Therefore the ^{19}F and proton relaxation times, $(T_{1p}^{-1})_F$ and $(T_{1p})_*$ respectively, obtained from competition experiments at various pH values should be related to F^-, N_3^- and OH^- concentrations according to the following general relationships:

$$(T_{1p})_F = (1 + K_{OH}[OH^-] + K_N[N_3^-] + K_F[F^-])/(AK_F E_0) \quad (1)$$

$$(T_{1p})_* = 1/BE_0 + (1 + K_F[F^-] + K_N[N_3^-])/(BE_0 K_{OH}[OH^-]), \quad (2)$$

where *A* and *B* are spectroscopic constants, K_F, K_N and K_{OH} indicate the stability constants of the complexes between MnSOD and F^-, N_3^- and OH^- respectively. These equations have been derived by developing a model for competition between different inhibitors (Lanir and Navon 1972; Viglino et al. 1979) and are valid in the condition $[F^-], [N_3^-] \gg E_0$.

The straight lines obtained by plotting $(T_{1p})_F$ vs. $[OH^-]$ or $(T_{1p})_*$ vs. $[OH^-]^{-1}$, see Figs. 2b and 4b respectively, strongly support the proposed model and, according to Eqs. (1) and (2), a K_{OH} value of $1.1 \times 10^{-4} M^{-1}$ was calculated from the ratio intercept/slope. Similarly the straight lines obtained by plotting $(T_{1p})_F$ or $(T_{1p})_*$ vs. the concentration of the inhibitors at constant pH values gives the stability constant K_F and K_N reported in Table 1.

The consistency between ^{19}FMR and PMR data is confirmed by the theoretical curves, broken line of Fig. 2 a and full line of Fig. 4 a, calculated by introducing the stability constant values of Table 1 in Eqs. (1) and (2) respectively. These curves fit the experimental data at pH values below 10.3 very well. Above pH 10.3 a progressive divergence between experimental data and theoretical curves takes place; such disagreement can be correlated with a progressive modification of the active site structure, most likely due to the titration of neighbouring charged aminoacid residues. The changes of the dynamics and the structure of site *B*, occurring above pH 10.3, are also well documented by the data of Fig. 1 and Table 1, which show the variations of the values of the stability constants and of the relaxation parameters occurring at pH 10.5.

The small effect of saturating amounts of N_3^- on PMR at neutral pH and on the asymptotic $(T_{1p}^{-1})_\infty$ value at alkaline pH values, could be due to a moderate conformational distortion of the Mn(III) ligand field which affects the T_{1p} of H_2O bound at site *A* when N_3^- binds at site *B*, or to the binding of a second N_3^- molecule to site *A* with a stability constant much less than K_N. Analogous effects have been suggested in the case of Cu, Zn superoxide dismutase (Bertini et al. 1981).

Our experimental data do not permit an unambiguous assignment of the O_2^- coordination site. NMR data indicate the anion coordination is at site *B* and could suggest an analogous coordination for O_2^-, as

anion, while activity measurements are more difficult to explain. In fact the azide inhibition does not appear to be competitive with respect to O_2^- (Misra and Fridovich 1978) while the slight inhibition of the activity by F^- could be ascribed to ionic strength effects (Argese et al. 1987).

The pH dependence of the enzyme activity, reported by McAdam et al. (1977b), shows a gradual decrease of the rate constant above pH 8 which could be due to O_2^- coordination at site *B* in competition with OH^-; nevertheless it has been demonstrated that, in the case of the Cu, Zn superoxide dismutase (Argese et al. 1987), the titration, at increasing pH values, of positively charged groups near the active site is the factor which decreases the activity of the enzyme. In conclusion, our experimental data do not permit us, at present, to determine which of the two effects is the one operating on the enzyme activity.

References

Argese E, Viglino P, Rotilio G, Scarpa M, Rigo A (1987) Electrostatic control of the rate determining step of the copper, zinc superoxide dismutase catalytic reaction. Biochemistry 26: 3224–3228

Bertini I, Borghi E, Luchinat C, Scozzafava A (1981) Binding sites of anions in superoxide dismutase. J Am Chem Soc 103:7779–7783

Brock CJ, Walker JE (1980) Superoxide dismutase from *Bacillus stearothermophilus*. Metal binding and complete amino acid sequence. In: Bannister JV, Hill HAD (eds) Developments in biochemistry, vol 11a. Elsevier North Holland, New York, pp 237–241

Brock CJ, Harris JI, Sato S (1976) Superoxide dismutase from *Bacillus stearothermophilus*. Preparation of stable apoprotein and reconstitution of fully active enzyme. J Mol Biol 107:175–178

Dwek RA (1973) NMR in biochemistry: applications to enzyme systems. Clarendon Press, Oxford, pp 174–212

Fee JA, Shapiro ER, Moss TH (1976) Direct evidence for Manganese(III) binding to the manganosuperoxide dismutase of *Escherichia coli B*. J Biol Chem 251:6157–6159

Gerritsen HJ, Sabisky ES (1963) Paramagnetic resonance of trivalent manganese in rutile (TiO_2). Phys Rev 132:1507–1512

Lanir A, Navon G (1972) Nuclear magnetic resonance studies of carbonic anhydrase. Binding of sulfacetamide to the manganese enzyme. Biochemistry 11:3536–3543

Luz Z, Meiboom S (1964) Proton relaxation in dilute solutions of Cobalt(II) and Nickel(II) ions in methanol and the rate of methanol exchange in the solvation sphere. J Chem Phys 40:2686–2692

McAdam ME, Fox RA, Lavelle F, Fielden M (1977a) A pulse-radiolysis study of the Manganese containing superoxide dismutase from *Bacillus stearothermophilus*. A kinetic model for the enzyme action. Biochem J 165:71–79

McAdam ME, Lavelle F, Fox RA, Fielden M (1977b) A pulse-radiolysis study of the Manganese containing superoxide dismutase from *Bacillus stearothermophilus*. Further studies on the properties of the enzyme. Biochem J 165:81–87

McCord JM, Fridovich I (1969) Superoxide dismutase, an enzymic function for erythrocuprein. J Biol Chem 244: 6049–6055

Misra PH, Fridovich I (1978) Inhibition of superoxide dismutases by azide. Arch Biochem Biophys 189:317–322

Pick M, Rabani J, Yost F, Fridovich I (1974) The catalytic mechanism of the manganese containing superoxide dismutase of *Escherichia coli* studied by pulse radiolysis. J Am Chem Soc 96:7329–7332

Stallings WC, Pattridge KA, Strong RK, Ludwig ML (1985) The structure of manganese superoxide dismutase from *Thermus thermophilus HB8* at 2.4 A resolution. J Biol Chem 260: 16422–16432

Viglino P, Rigo A, Stevanato R, Ranieri GA, Rotilio G, Calabrese L (1979) The binding of fluoride ion to bovine cuprozinc superoxide dismutase as studied by ^{19}F magnetic relaxation. J Magn Reson 34:265–274

Villafranca JJ, Yost FJ, Fridovich I (1974) Magnetic resonance studies of manganese(III) and iron(III) superoxide dismutases. J Biol Chem 249:3532–3536

Walker JE, Auffret AD, Brock CJ, Steinman HM (1980) Structural comparisons of superoxide dismutases. In: Bannister JV, Hill HAO (eds) Developments in biochemistry, vol 11a. Elsevier North Holland, New York, pp 213–222